Meteoritics & Planetary Science 40, Nr 1, 35–54 (2005)
Abstract available online at http://meteoritics.org

Fragmentation model of meteoroid motion, mass loss, and radiation in the atmosphere

Zdeněk CEPLECHA[1*] and Douglas O. REVELLE[2]

[1]Academy of Sciences of the Czech Republic, Astronomical Institute, Observatory, 25 165 Ondřejov, Czech Republic
[2]Los Alamos National Laboratory, P.O. Box 1663, MS D401, Earth and Environmental Sciences Division, EES-2, Atmospheric and Climate Science Group, Los Alamos, New Mexico 87545, USA
*Corresponding author. E-mail: zdenekce@asu.cas.cz

(Received 3 October 2003; revision accepted 24 November 2004)

Abstract–We present the basic differential equations of meteor physics (the single body equations). We solve them numerically including two possible types of fragmentation: into large pieces and into a cluster of small fragments. We have written a Fortran code that computes the motion, ablation and light intensity of a meteoroid at chosen heights, and allows for the ablation and shape density coefficients σ and K, as well as the luminous efficiency τ, to be variable with height/time. We calibrated our fragmentation model (FM) by the best fit to observational values for the motion, ablation, radiation, fragmentation and the terminal masses (recovered meteorites) for the Lost City bolide. The FM can also handle multiple and overlapping meteor flares. We separately define both the apparent and intrinsic values of σ, K, and τ. We present in this paper values of the intrinsic luminous efficiency as function of velocity, mass, and normalized air density. Detailed results from the successful application of the FM to the Lost City, Innisfree, and Benešov bolides are also presented. Results of applying the FM to 15 bolides with very precise observational data are presented in a survey mode (Table 7). Standard deviations of applying our FM to all these events correspond to the precision of the observed values. Typical values of the intrinsic ablation coefficient are low, mostly in the range from 0.004 to 0.008 s^2 km^{-2}, and do not depend on the bolide type. The apparent ablation coefficients reflect the process of fragmentation. The bolide types indicate severity of the fragmentation process. The large differences of the "dynamic" and "photometric" mass from numerous earlier studies are completely explained by our FM. The fragmentation processes cannot be modeled simply by large values of the apparent ablation coefficient and of the apparent luminous efficiency. Moreover, our new FM can also well explain the radiation and full dynamics of very fast meteoroids at heights from 200 km to 130 km.

INTRODUCTION

In this work, we have developed a new fundamental data analysis technique to completely examine the nature of the atmospheric interaction with a meteoroid traveling at hypersonic velocities during entry. This technique includes simultaneously the effects of luminosity, fragmentation, ablation, and entry dynamics. Earlier Ceplecha et al. (1993) examined the relationship between fragmentation, ablation, and bolide entry dynamics using the most precise data available. With the recent detailed analyses of the Lost City meteorite fall, we have now established a fully calibrated luminous efficiency parameter (in a panchromatic passband) as a function of mass, velocity, and air density that has allowed the bolide luminosity production to be added to the data analysis procedure developed earlier. Our analysis naturally leads to the concepts of the intrinsic versus the apparent values of the ablation coefficient and of the luminous efficiency parameter. Apparent values of these parameters are the single body values uncorrected for the effects of fragmentation, while the intrinsic values are the apparent values after correction for the dominant effects of fragmentation. Using this new procedure, after certain assumptions about the sizes of the fragments relative to the main leading entry mass have been made, we have been able to completely analyze bolides of all possible types including even IIIB bolides, whose fundamental nature has always been extremely difficult to understand. As a result of our work, the paradox of the computed large difference between the photometric and dynamic mass has now been completely resolved.

METEOR PHYSICS

The term "meteor physics" was invented many decades ago to distinguish the pure descriptive approach of observing meteors from the studying of the interaction of meteoroids with the atmosphere. Equations based on the simplest physical principles are well capable of describing processes giving rise to meteors, to meteoric fireballs (bolides), and to superbolides. Thus, the term "meteor physics" seems to be somewhat superfluous. Before sufficiently precise observing techniques were used, any physical approach had been just speculative. Recording meteors with photographic cameras and later by radars and TV cameras, made a substantial change in the situation. Observational records are capable of: a) yielding very precise geometrical data on the atmospheric trajectory of a meteoroid; and b) by converting theoretical concepts into ready tools, such records can also be utilized to explain numerous aspects of meteoroid motion, ablation, fragmentation, and luminosity.

Given our current knowledge regarding the details of meteoroid interactions with the atmosphere, we can, in principle, develop sophisticated models of a meteor after specifying the meteoroid's initial properties. All of our theoretical concepts for meteoroid motion and ablation are based on simple physics. This means that only an exchange of energy and conservation of momentum of a meteoroid driving forward into the atmosphere have been assumed in deriving the basic differential equations, sometimes also called the "single body theory." During the sixty-year period that this concept has been used, there has not been a substantial change in the form of the equations (but rather in their interpretations) since comparatively simple physics can be used to fit our most precise observations available with residuals corresponding to a geometrical precision of these observations (±20 m is a typical precision in lateral distances measured along a meteoroid trajectory). Much more precise observations may call for a new formulation of the basic differential equations, but this does not seem possible yet.

Fragmentation is a very important phenomenon, which complicates any application of the single body theory to observations of meteors. There are two basic fragmentation phenomena recognized: a) continuous fragmentation (which is actually the main process of meteoroid ablation); and b) sudden fragmentation (at "a point"; also referred to as gross fragmentation or discrete fragmentation). The term meteoroid ablation means all mass leaving the body (mass loss) and we do not distinguish whether or not this mass removal is realized as gaseous/vapor, liquid droplets, or solid fragments. Distinguishing these forms of ablation with precise observations alone is not possible, except in the case of discrete fragmentation. We know that most of the ablation occurs in small fragments because the apparent ablation coefficients that we compute for individual meteoroids from their precise observations are much larger values than that corresponding to evaporation, sublimation, or spraying of droplets from a molten meteoroid surface.

How much light is radiated—compared to the total kinetic energy or to the time change of kinetic energy due to ablated mass and to the deceleration—has been one of the most speculative parts of the physical theory of meteors so far. Luminous efficiencies used by many authors are based on some very old computations (Öpik 1933, 1955) with experimental calibration for masses of about 1 gram (Ayers et al. 1970). These values are presumed to be a function of velocity only, while through physics one may reason that luminous efficiencies should significantly depend on several other values, e.g., the mass of the body, the density of the atmosphere, etc. When modeling trajectories of different fragments of the photographically-recorded Innisfree meteorite fall, Halliday et al. (1978, 1981) found an explicit dependence of the luminous efficiency on mass. They also found larger values of luminous efficiency than were traditionally used by many investigators to derive meteoroid masses. Recent studies of the Lost City bolide (Ceplecha 1996) yielded an apparent luminous efficiency of about 6%, while the values used for the initial interpretation of the majority of the Prairie Network meteors were assumed to be below 1% at the same velocity. Such values of the apparent luminous efficiency were derived from precise photographic observations by means of the single body equations without proper handling of fragmentation. In this paper, we have renamed these uncorrected values as the "apparent luminous efficiency". "Intrinsic luminous efficiency" is what we shall call the values of luminous efficiency that are derived from a proper model of fragmentation added to the basic differential equations of meteor physics.

At this point, we want to stress that in this paper we dealt with precise photographic data by making use of panchromatic emulsions. Our luminous efficiencies are entirely related to the panchromatic passband, which corresponds mostly to the metal atom line emissions. Calibrations were mostly done by the Lost City, Innisfree, and Benešov fireballs. Thus, our results on high velocity fireballs (e.g., Leonids) should be taken as provisional, though they are as good as the results on slow-moving fireballs. Absolute calibrations for high velocity meteoroids require future work.

In this paper, we take the approach of combining the fundamental equations of meteor physics with some of the best observational dynamic and light curve data available. We utilize data from 15 very precisely observed bolides, which include data from three very significant fireballs (two of which dropped recovered meteorites with significant ground truth information), namely Lost City, Innisfree, and the famous Czech bolide Benešov (which probably also dropped meteorites that were never recovered because of the locally steep and heavily forested terrain). Thus, we have used the fundamental single body equations combined with specific

relations developed for the analysis of fragmentation effects (for two types of proposed fragmentation processes, namely due to small and large fragments, respectively) to make detailed comparisons with the best available bolide observations.

Babadzanov (1991) was one of the first to properly include fragmentation effects in explaining the precise photographic observations of meteor phenomena. His method was aimed at obtaining meteoroid densities through statistical methods yet based on fitting individual events to a theoretical concept of quasi-continuous fragmentation. His findings that meteoroids belonging to different streams possess approximately the same values of bulk densities as sporadic meteoroids, and that the values of densities are inside the range of densities of meteorites, are somewhat similar to results of this paper, except that we are reluctant to assign densities to individual meteoroids of unknown shape. However, Babdzanov used apparent luminous efficiencies, and thus a direct comparison of our results with those of Babadzanov is not possible. Nevertheless, our mathematical description of the fragmentation processes is quite different from that of Babadzanov and has led us to reveal the important distinction between intrinsic values of the luminous efficiency and the apparent values, which solved the long-lasting enigma of dynamic versus photometric mass in interpreting precise photographic data on meteors.

In a companion paper first presented in Kiruna (at Meteoroids 2001) and later refined and presented at the ACM in Berlin (ReVelle 2002), a similar analysis was also presented for bolides in cases of either uniform bulk density or uniform volume-weighted porosity using a theoretical model of the convective/conductive (for turbulent/laminar "gas cap" boundary layer flow, respectively) and also of the radiative heat transfer coefficients that form the numerator of the ablation parameter. In this model, we also included a similar model of triggered progressive fragmentation into a geometric cascade of fragments that continued until the termination of the flight (unless it was terminated earlier using observational constraints directly available from flight data). Following the progressive fragmentation process (only triggered if the stagnation pressure exceeded the bolide's presumed strength as a function of the bolide type or the degree of assumed porosity), the released fragments were either "lost" to the wake or allowed to interact with the main leading fragment dynamically and energetically. Apparent values of the ablation parameter and of the luminous efficiency were used directly to produce specific dynamic and energetics predictions (including fragmentation) as well as the panchromatic luminous emission expected for a specific bolide. As expected from the work presented directly in this paper, the predicted ablation parameter decreased during these fragmentation events. This decrease in the ablation parameter was produced because the smaller resultant fragment sizes have smaller predicted heat transfer coefficients regardless of the specific heat transfer mechanism type. Generalized expressions for prediction of the single body and of the fragmentation-dominated regimes of flight (through a comparison of the fragmentation scale height against the density (pressure) scale height) were also identified therein. The key point here is that we are now rapidly converging on a solution to this problem from two independent and combined viewpoints. Agreement between these two independent approaches for the initial mass for Benešov, for example, is outstanding, as is also the case for the Lost City bolide. For Innisfree, the analysis has not yet been formally redone using the approach given in ReVelle (2002), but all expectations are that it will also agree quite well with the approach discussed in detail below.

Basic Differential Equations of Meteor Physics (Single Non-Fragmenting Body or Single Body Theory)

The ablation and motion of a single non-fragmenting body through the atmosphere can be given by three fundamental differential equations, assuming a linear trajectory, ballistic entry neglecting lift forces and gravity, and Earth's surface approximated by an osculating sphere (Ceplecha et al. 1993, 1998):

$$\frac{dv}{dt} = -K\rho m^{-1/3} v^2 \tag{1}$$

$$\frac{dm}{dt} = -K\sigma\rho m^{2/3} v^3 \tag{2}$$

$$I = -\tau\left(1 + \frac{2}{\sigma v^2}\right)\frac{v^2}{2}\frac{dm}{dt} \tag{3}$$

$$\frac{dh}{dt} = \frac{1 - A/2}{B/2 + h} v \tag{4}$$

$$\frac{A/2 - l}{B/2 + h} = \cos z(t) \tag{5}$$

$$Al + Bh + C = l^2 - h^2 \tag{6}$$

Equations 1, 2, and 3 are usually referred to as drag, mass loss, and luminous equations, respectively. Equation 1 represents conservation of momentum and Equation 2 expresses conservation of kinetic energy. Equation 4 defines the geometry of the trajectory, i.e., relation of distances along the trajectory l as function of height h. The two independent parameters of the problem, the ablation coefficient σ and the shape density coefficient K, are defined by the following expressions:

$$\sigma = \frac{\Lambda}{2\zeta\Gamma} \tag{7}$$

$$K = \Gamma A' \rho_d^{-2/3} \tag{8}$$

The third independent parameter τ is the differential luminous efficiency (the apparent differential luminous efficiency in case of not accounting properly for all fragmentation). For a meteoroid at an arbitrary point of its trajectory, the notation has the following meaning: v = velocity; t = time (independent variable); m = mass; I = meteor luminosity; h = height; l = distance along the trajectory; ρ = air density; z = zenith distance of the radiant (slope to vertical); Γ = drag coefficient; Λ = dimensionless heat transfer coefficient; $A' = Sm^{-2/3}\rho_d^{2/3}$ = shape factor; S = head-cross section; ρ_d = bulk density of the meteoroid; ζ = energy necessary for ablation of a unit mass; and A, B, and C are constants of the geometrical position of the trajectory (a straight line over a sphere) and can be expressed as:

$$A = 2l_0 + 2R\cos z_0 + 2h_0\cos z_0 \tag{9}$$

$$B = 2R \tag{10}$$

$$C = -l_0^2 - 2Rh_0 - h_0^2 - 2Rl_0\cos z_0 - 2h_0 l_0\cos z_0 \tag{11}$$

where R is the radius vector from the Earth's center to the geographical location at the Earth's surface ($h = 0$) belonging to the point $l = l_0$, $h = h_0$; and z_0 is the zenith distance of the radiant (slope of the trajectory to the vertical line) at the point l_0, h_0. Because the distance along the trajectory l is a relative distances, we can chose $l_0 = 0$, i.e., starting to determine distances along the trajectory from the height h_0. Then, the above equations defining A, B, C convert to somewhat simpler expressions:

$$A = 2R\cos z_0 + 2h_0\cos z_0 \tag{9a}$$

$$B = 2R \tag{10a}$$

$$C = -2Rh_0 - h_0^2 \tag{11a}$$

Having values of h and l available at three or more points of the trajectory, Equation 6 can be used for computing A, B, C. If we know the slope of the trajectory to vertical z_0 at the point where $h = h_0$, we can compute A, B, C from Equations 9a, 10a, and 11a. The relationship of A, B, C to z_0 can be expressed as:

$$\cos z_0 = \frac{A/2}{\sqrt{B^2/4 - C}} \tag{12}$$

If the height of an arbitrary point on the meteor trajectory is h, then the corresponding distance along trajectory at the same point l is given by:

$$l = A/2 - \sqrt{A^2/4 + C + h^2 + Bh} \tag{13}$$

If the distance along the trajectory at an arbitrary point is l, then the corresponding height at the same point h is given by:

$$h = -B/2 + \sqrt{B^2/4 - C + l^2 - Al} \tag{14}$$

Equation 14 is valid before the closest point to the Earth's surface, i.e., for h decreasing with increasing l, which is the normal situation for the vast majority of events. In an exceptional case of a meteor observed after its perigee (h increases with increasing l), the sign of the square root in Equation 13 must be then taken to be positive.

FRAGMENTATION MODEL (FM)

We assume that a flare on a meteor light curve represents a discrete fragmentation event. We use the term gross fragmentation rather in sense of separation of a large fragment from the main body at a fragmentation height (point) on the meteoroid trajectory. This also relates to some older work (Ceplecha et al. 1993) based on dynamic behavior of meteoroids, where the mathematical handling allows for just one separation height—the gross fragmentation height. By major disruption we mean a discrete fragmentation event with a decisive meaning for the mass loss of the main body.

The solution of Equations 1, 2, and 4 assuming constant K and σ was presented in Ceplecha et al. (1998). We will follow this solution in describing individual steps of our fragmentation model (FM) that we have programmed in Fortran. A numerical solution by means of a step-by-step integration of the basic equations seems to be the only way in which the complicated phenomenon of fragmentation can be included into the basic differential Equations 1–4.

Motion, Ablation, and Radiation of the Main Body

$$\Delta h = h_2 - h_1 \tag{15}$$

$$\mathrm{Ei}\left(\frac{\sigma_1 v_2^2}{6}\right) = \mathrm{Ei}\left(\frac{\sigma_1 v_1^2}{6}\right) + 2K_1\rho(h_1)\exp\left(\frac{\sigma_1 v_1^2}{6}\right)m_1^{-1/3}\cos^{-1}z(h_1)\Delta h \tag{16}$$

where $\mathrm{Ei}(x)$ is the exponential integral defined by $\mathrm{Ei}(x) = \int_{-\infty}^{x} u^{-1}\exp(u)\mathrm{d}u$. Making use of the exponential integral function inside our code makes it about 6× speedier. Equation 16 was derived assuming that both K and σ are constants. Thus, after computation over a sufficiently small height interval, Δh (in practice, 0.01 km has been used most) and assuming constant K and σ within this interval, these variables are assigned numerical values corresponding to the start of the interval. The subscript 1 relates to the beginning of the integration interval (Δh), and the subscript 2 relates to the end of the integration interval (Δh). The variables denote the following: h = height, v = velocity, m = mass, ρ = air density,

z = zenith distance of the radiant (the deviation of the trajectory from local vertical line), σ = ablation coefficient, K = shape density coefficient. Equation 16 allows the computation of v_2 from v_1, and all of the other known values at the beginning of the integration interval (subscript 1). In the code, care is also taken of very shallow near horizontal trajectories: the code recognizes when a meteoroid passes beyond the perigee point and the height then starts to increase. Knowing v_2, we can now compute m_2 from the following equation (Ceplecha et al. 1998):

$$m_2 = m_1 \exp\left[\frac{\sigma_1}{2}(v_2^2 - v_1^2)\right] \quad (17)$$

Deceleration and mass loss at the end of the integration interval (subscript 2) can be computed from Equations 1 and 2 written in the form of Equations 18 and 19:

$$\left(\frac{dv}{dt}\right)_2 = -K\rho(h_2)m_2^{-1/3}v_2^2 \quad (18)$$

$$\left(\frac{dm}{dt}\right)_2 = \sigma_2 m_2 v_2 \left(\frac{dv}{dt}\right)_2 \quad (19)$$

Luminous intensity I_2 is then given by Equation 3 written as Equation 20. If velocity is expressed in cm/s and mass in g, the result is in erg/s:

$$I_2 = -\tau_2\left(1 + \frac{2}{\sigma_2 v_2^2}\right)\frac{v_2^2}{2}\left(\frac{dm}{dt}\right)_2 \quad (20)$$

In order to convert from erg/s to Watts, Equation 20 must be multiplied by 10^{-7}. For conversion to absolute stellar magnitude M_2 (for a source at an altitude of 100 km in the zenith, assuming isotropy), we have the following Equation (Ceplecha et al. 1998):

$$M_2 = -2/5\ (\log I_2 - 10.185) \quad (21)$$

where I_2 is expressed in erg/s and log is common (base 10) logarithm.

In order to relate v to h and t to h, we have to define the geometrical position of the trajectory. This is done by using distance l flown by the body along its trajectory. If the trajectory is a straight line over a sphere (the geoid osculation sphere at the body location), then the problem is defined by three constants *A, B, C* given by Equations 9a, 10a, and 11a. For any height h the distance along trajectory l is given by Equation 13 and z (slope of the trajectory to vertical) is given by Equation 12.

Gross Fragmentation Parameterizations

Two different types of fragmentation are accounted for separately: a) fragmentation into large fragments comparable in mass to the main body; and b) fragmentation into a cluster of small fragments. This is necessary because light emission from individual large fragments contributes to the light curve less than light emission from many small fragments (due to substantially smaller exposure surface).

Fragmentation into Several Large Fragments

We assume that several large fragments are liberated from the main body instantaneously at a trajectory point (height). We neglect the small time interval between the release of the fragments and the start of the emission of light. We assume that the fragments are large enough to remain rather close to the main body. We express the mass of the fragments in units of the main body mass. Thus, if we set the mass of the main body equal to 1 and mass of all the large fragments equal to n_F, this can be used to define the coefficient k_F by $k_F = 1 + n_F$. Multiplying the mass loss of the main body by this coefficient, we arrive at total mass loss of the main body and all the large fragments. Because this mass loss is proportional to the radiation produced, the radiated energy computed from Equation 20 for the main body, i.e., I_2, also has to be multiplied by k_F in order to obtain the radiation originating from all of the constituents remaining (large fragments and the main body). This assumes that the large fragments are so close to the main body that we cannot distinguish their radiation emission from that of the main body. Because large fragments are usually radiating for some shorter time than the main body, we have defined their lifetime within the code. The radiation of the main body and all large fragments is then represented in the code by the term $k_F I_2$.

Fragmentation into a Cluster of Small Fragments

We assume that many small fragments are liberated from the main body instantaneously at a trajectory point. However, they need some small time interval to heat up and start to ablate, and then they can fully contribute to the main body's luminosity. Such a time interval is assumed to be the interval from the start of a flare to the maximum of the flare and is denoted Δt_U. Having an observed light curve, it is relatively easy to determine this time interval. We also need the total duration of the flare, denoted Δt_F, a value also directly determinable from observations. The total mass liberated in form of small fragments at a flare is denoted m_F. The liberation of fragments $(dm/dt)_U$ and the following mass loss of fragments $(dm/dt)_F$ can be expressed as:

$$\left(\frac{dm}{dt}\right)_U = a\ \exp(-bt_F^2) \quad (22)$$

$$\left(\frac{dm}{dt}\right)_F = a\ \exp(-ct_F^2) \quad (23)$$

where t_F is relative time counted forward from the maximum of the flare ($t_F = 0$ at the maximum of the flare). Equations 22 and 23 were found as the best possible fit to the shape of the light curve for very small fragments released much deeper than they could normally penetrate the atmosphere by themselves. Such computational experiments were performed using a single body form of the code. We started very small meteoroids as single bodies deep in the atmosphere (this is equivalent to "to be released from a bigger body") and computed their radiation. Equations 22 and 23 contain 3 unknown values *a, b, c* to be determined. They are computed from a condition that $(dm/dt)_U$ must be negligible compared to mass loss $(dm/dt)_{MU}$ of the main body at the start of the flare. The second condition holds for the end of the flare, where also $(dm/dt)_F$ must be negligible according to the mass loss $(dm/dt)_{MF}$ of the main body. If suffix *M* denotes the main body value, *U* denotes start of the flare, and *F* denotes the end of the flare, the conditions can be written as:

$$\varepsilon\left(\frac{dm}{dt}\right)_{MU} = a\ \exp(-b\Delta t_U^2) \tag{24}$$

$$\varepsilon\left(\frac{dm}{dt}\right)_{MF} = a\ \exp[-c(\Delta t_F - \Delta t_U)^2] \tag{25}$$

where ε is an appropriately small value such that the light contribution from these fragments to the light contributed by the main body is already negligible.

The third necessary condition for computing *a, b, c* values is derived from a condition that conserves the total mass such that the integration of all mass loss of the fragments over the time of the flare must be equal to m_F, i.e., to the total mass of all released fragments:

$$m_F = a\int_0^{\Delta t_F - \Delta t_U} \exp(-ct^2)dt \tag{26}$$

This integral cannot be expressed exactly as a closed analytical expression. However, we found a new and very good approximation to Equation 26 given as Equation 27:

$$m_F = \frac{a\ \tanh[\sqrt{c}(\Delta t_F - \Delta t_U)]}{\sqrt{c}} \tag{27}$$

Equation 27 yields values closer than 1% to the exact value (numerically derived from Equation 26) for all intervals, which could be met in practical application to realistic meteoroid flares. Application of Equation 27 sped up our computations significantly. Now we can express the values of *a, b, c* as:

$$\frac{\varepsilon\left(\frac{dm}{dt}\right)_{MF}}{m_F} = \frac{\sqrt{c}\exp[-c(\Delta t_F - \Delta t_U)^2]}{\tanh[\sqrt{c}(\Delta t_F - \Delta t_U)]} \tag{28}$$

This equation can readily be solved for *c* numerically. Having *c*, we can determine *a* from:

$$a = \frac{m_F\sqrt{c}}{\tanh[\sqrt{c}(\Delta t_F - \Delta t_U)]} \tag{29}$$

and *b* from

$$b = \frac{-\ln\left[\frac{-\varepsilon\left(\frac{dm}{dt}\right)_{MU}}{a}\right]}{\Delta t_U^2} \tag{30}$$

Having values of *a, b, c*, the mass loss can be determined from Equations 22 and 23 and the contribution to the light curve can be computed from Equation 20.

Fragmentation Overlapping the Duration of the Preceding Flare

Such an event does not require any special mathematical formulation. One should only keep each fragmentation event independently contributing to the light curve, i.e., keep the current t_F definition and *a, b, c* definitions, and also using the k_F definition for each fragmentation point individually and independently working until $t_F = \Delta t_F - \Delta t_U$. The sum of all radiation contributions added to the emission of radiation from the main body (including radiation from large fragments) forms the total light curve with all overlapping flares taken into account. This is a somewhat difficult procedure in practice, because we need to recognize the regions of increasing and decreasing values of (dm/dt), i.e., if either Equation 22 or 23 is valid for the integration step currently being computed.

Intrinsic Values of σ, *K*, and τ

Values of the coefficients, as defined in the section Motion, Ablation, and Radiation of the Main Body, are the values without fragmentation explicitly included in the computations. If these single body equations were applied to bolide data observed for a bolide with fragmentation (i.e., applied without accounting for the fragmentation), apparent values of σ, *K*, and τ will result. If the fragmentation is properly accounted for, values of σ, *K*, and τ have then been corrected for fragmentation, and we will term them their intrinsic values. Our model will allow for the first time to use direct observations to compute the intrinsic values of σ, *K*, and τ (i.e., their values corrected for both forms of fragmentation that we have parameterized earlier).

Now that we recognized the importance of the two different types of fragmentation for the interpretation of bolide observations (large fragments, clusters of small fragments),

we will propose using a new terminology to describe the situation. We will recognize two different sets of σ, *K*, and τ values—apparent and intrinsic—according to the following definitions:

- The apparent values of σ, *K*, and τ are those computed from observational (dynamic and photometric) data of the main body neglecting the fragmentation process. Such values were used in most studies so far (e.g., Ceplecha 1988), and also for interpretation of the Lost City bolide observations (e.g., Ceplecha 1996).
- The intrinsic values of σ, *K*, and τ are those computed from observational (dynamic and photometric) data of the main body, including the fragmentation process. These intrinsic values are the apparent values corrected for the effects of fragmentation.

NUMERICAL INTEGRATION OF FM EQUATIONS

Input Values for the FM

Before computation of all relevant parameters from a well-observed bolide event, one has to prepare an assumed fragmentation pattern containing data on heights and where the gross fragmentation (flare) occurred. The number of such points is not limited in our code. Each fragmentation point is defined by: 1) height of the fragmentation point h_F; 2) percent of mass of the main body lost at the fragmentation point; 3) time duration, Δt_F, of the flare (this is time span from the start of the flare until its end where all fragments are already completely consumed, i.e., where they cease adding luminosity to the main body radiation); 4) time interval Δt_U, from the start of the flare until the flare maximum; 5) the definition of a new value of the intrinsic shape density coefficient *K*: this represents a sudden change of the shape of the main body at the fragmentation height; 6) definition of a new value of the intrinsic ablation coefficient σ (this represents a sudden change of intrinsic ablation coefficient of the main body at the fragmentation height); and 7) part of the mass fragmented as large fragments (comparable in mass to the main mass) in terms of the percent of all fragmented mass at the fragmentation height.

Initial Values for the Integration

The computation starts with $t_1 = 0$, $l_1 = 0$, i.e., time and distance along the trajectory are taken to be zero at the start of computation. The input file defines: h_1 = the beginning height; z_1 = the slope of the trajectory to the vertical at h_1; v_1 = the velocity at h_1; m_1 = the mass at h_1; K_1 and σ_1 are set to initial values valid before the first fragmentation point; intrinsic τ_1 is computed from a subroutine as function of v_1, m_1, h_1, ρ_1; $(dv/dt)_1$ is computed from Equation 18 with subscript 1; $(dm/dt)_1$ is computed from Equation 19 with subscript 1; I_1 is computed from Equation 20 with subscript 1; M_1 is computed from Equation 21 with subscript 1. The integration height interval is prescribed as Δh.

Integration Step (from Subscript 1 to Subscript 2)

h_2 is computed by subtracting the integration height interval Δh; l_2 is computed from Equation 13; v_2 is computed from Equation 16; cos z_2 is computed from Equation 12 with h_2, l_2; time step Δt_1 corresponding to the assumed Δh value is computed from l_1, l_2, v_1, v_2: $\Delta t_1 = 2(l_2 - l_1)/(v_1 + v_2)$; $t_2 = t_1 + \Delta t_1$; m_2 is computed from Equation 17; and K_2 and σ_2 are set to the actual values as prescribed in the input file; the intrinsic τ_2 is computed from a subroutine as a function of v_2, m_2, h_2, ρ_2, i.e., from Equations 31 and 32, or from Equations 33 and 34; $(dv/dt)_2$ is computed from Equation 18; $(dm/dt)_2$ is computed from Equation 19; I_2 is computed from Equation 20; I_F originating from fragments is added; M_2 is computed from Equation 21.

Preparing for Repetition of the Integration Step

Values with subscript 1 are overwritten by values with subscript 2, i.e., values of cos *z, t, l, h, v, m, K,* σ, and τ. The procedures in the sections Integration Step (from Subscript 1 to Subscript 2) and Preparing for Repetition of the Integration Step are continuously repeated until computation ceases due to low velocity (≈3 km s^{-1}), or because of very low mass or very low brightness.

Gross Fragmentation

If gross fragmentation takes place at a prescribed height h_F, then t_F is defined as $t_F = -\Delta t_U$; the fragmented mass m_F is computed from the mass of the main body m_2 and from the percent of the mass of the main body being fragmented; the new mass m_2 of the main body is computed; the mass of the large fragments is computed; k_F is determined; the part of the fragmented mass that becomes small fragments is computed; K_2, σ_2, τ_2 values for the gross fragmentation event (flare) are determined; Equation 28 is solved for *c*; *a* is computed from Equation 29 and *b* from Equation 30; the ascending part of the flare starts to be used for the mass loss of the fragments computed from Equation 22; the mass loss of all preceding fragmentation events still available (if any) for the light emission is added to the mass loss of the actual fragmentation event; then I_F the intensity of light from all active fragmentation events is computed; the time step Δt_1 is added to the t_F of the actual fragmentation event, and also added to all preceding and still active fragmentation events; either the increasing wing of the flare represented by Equation 22 or the decreasing wing of the flare represented by Equation 23 are used for computing the actual value of $(dm/dt)_U$ or $(dm/dt)_F$, respectively; the descending part of the actual flare (i.e., the entire flare or the gross fragmentation event itself) is

terminated by the condition that t_F is greater than $\Delta t_F - \Delta t_U$; finally, the total computation of the light contribution follows with the addition of I_F to I_2.

INTRINSIC LUMINOUS EFFICIENCY

Applying our model to the Lost City observational data, i.e., to the observed height as function of time and the observed light curve, we were also able to derive the corrections to the apparent luminous efficiencies previously published by Pecina and Ceplecha (1983) and revised by ReVelle and Ceplecha (2001). In order to fit the observational data to the Lost City bolide, we derived the intrinsic luminous efficiency as a function of the velocity v, mass m, and the normalized air density ρ/ρ_M, where ρ is the instantaneous air density at height h, and ρ_M is the air density at the height of maximum light of the bolide. The result is given by Equations 31 and 32.

If $v < 25.372$ km s^{-1},

$$\ln \tau = -1.230 - 10.307 \ln v + 9.781 \ln^2 v - 3.0414 \ln^3 v + 0.3213 \ln^4 v + 0.40 \tanh (0.38 \ln m) - 0.64 \ln (\rho/\rho_M) - 0.24 \ln^2 (\rho/\rho_M) - 0.029 \ln^3 (\rho/\rho_M) - 0.0016 \ln^4 (\rho/\rho_M) \quad (31)$$

It is assumed that Equation 31 holds for velocities less than 25.372 km s^{-1} analogous to the apparent τ derived earlier (ReVelle and Ceplecha 2001). Using the same approach, Equation 32 expresses the intrinsic τ for velocities greater or equal to 25.372 km s^{-1}:

If $v \geq 25.372$ km s^{-1}, then

$$\ln \tau = -3.226 + \ln v + 0.40 \tanh (0.38 \ln m) - 0.64 \ln (\rho/\rho_M) - 0.24 \ln^2 (\rho/\rho_M) - 0.029 \ln^3 (\rho/\rho_M) - 0.0016 \ln^4 (\rho/\rho_M) \quad (32)$$

τ in Equation 20 and 21 is expressed in percent of the first time derivative of the total kinetic energy, v is expressed in km s^{-1} and m is expressed in kg.

We were also able to derive similar expressions using a normalization of the instantaneous air density by the air density ρ_B, at the bolide beginning height h_B. Both results yielded almost identical residuals, however, Equation 33 gives somewhat smaller values of τ for the early parts of the trajectory close to the beginning height (see Fig. 1).

If $v < 25.372$ km s^{-1}, then

$$\ln \tau = -2.400 - 10.307 \ln v + 9.781 \ln^2 v - 3.0414 \ln^3 v + 0.3213 \ln^4 v + 0.40 \tanh (0.38 \ln m) + 0.46 \ln (\rho/\rho_B) - 0.073 \ln^2 (\rho/\rho_B) + 0.015 \ln^3 (\rho/\rho_B) - 0.0013 \ln^4 (\rho/\rho_B) \quad (33)$$

If $v \geq 25.372$ km s^{-1}, then

$$\ln \tau = -4.396 + \ln v + 0.40 \tanh (0.38 \ln m) + 0.46 \ln (\rho/\rho_B) - 0.073 \ln^2 (\rho/\rho_B) + 0.015 \ln^3 (\rho/\rho_B) - 0.0013 \ln^4 (\rho/\rho_B) \quad (34)$$

ANALYSIS OF THE LOST CITY BOLIDE (PN 40590)

Gross Fragmentation Model

A gross fragmentation solution (only dynamic data applied, the light curve not used) of the Lost City bolide was published by Ceplecha (1996) and contains two recognized gross fragmentation heights. The values of σ and τ in the cited paper are what we are now terming their apparent values. The value of K is intrinsic because the separation of $\Gamma A'$ from K was possible (since the meteorite densities are known from the ground truth information), and also the separation of Γ from A' was possible (a flat shape and rotation effects were also both recognized). The results are given in Table 1.

Results from the FM Applied to the Lost City Bolide

With the following values, we were able to fully explain the dynamics (height as function of time) and the light curve of PN 40590, the Lost City bolide and its associated meteorite falls. Large fragments and clusters of small fragments were both necessary for our FM best fit. Intrinsic $\sigma = 0.008$ s^2 km^{-2} intrinsic $K = 0.46$ c.g.s.; intrinsic τ given by Equation 31; $\varepsilon_h = \pm 13$ m, where ε_h is the standard deviation for one measured height; for ε_h as function of time see Fig. 6; $v_1 = 14.1486 \pm 0.014$ km s^{-1}; $m_1 = 165 \pm 6$ kg; $\varepsilon_M = \pm 0.17$ magnitudes; ε_M is the standard deviation for one measurement of brightness expressed in stellar magnitudes; for ε_M as function of time see Fig. 5. The resulting fragmentation heights and the amount of fragmentation of both types (large fragments, a cluster of fragments) is given in Table 2, where h_f is the height of a specific fragmentation point, Δm is mass loss at this height in the form of fragments of any size expressed in percent of the main body mass, dt_f is the duration of the flare, and dt_u is the time of increasing brightness of the flare, and Δm_F is the part of Δm fragmented as large fragments expressed in percent of Δm. The fragmentation heights with large Δm_F resulting from our FM (Table 2) are compared in Table 3 with separation heights of fragments derived from: a) intersection of individually observed trails; b) dynamic solution for the main body; and c) dynamic solution for the main body with a corresponding fragment (Ceplecha 1996). Also, dynamically derived masses are compared to masses resulting from our FM. The mass of the main body at the terminal point computed from our model is equal to 10.3 kg, compared to the mass at the terminal point determined from the dynamic solution that is equal to 9.8 kg, and compared to mass of the largest recovered meteorite (belonging to the main body trajectory) that is equal to 9.83 kg. The terminal velocity from our FM is 3.5 km s^{-1}, exactly equal to the value resulting from the dynamic solution (3.5 km s^{-1}). All these data proved the internal consistency of the FM and the derived intrinsic τ values that are predicted using Equation 31. Results of our FM analysis are plotted against time in Figs. 2–9. Results for

Table 1. The Lost City bolide and meteorite falls: model of gross fragmentation (Ceplecha et al. 1993) and rotation (Adolfson, forthcoming) applied to observed distances and heights as function of time.

Precision of two independent least-squares fits on partly superposing time intervals (135 measured points): standard deviation for one measured point without rotation ±21 m; standard deviation for one measured point including rotation ±18 m.		
Initial velocity		14.1485 ± 0.0012 km
Apparent ablation coefficient	from	0.0146 ± 0.0004
	to	0.0114 ± 0.0003
Mass	at the beginning height	163 ± 5 kg
	at the terminal height of the main body	9.79 ± 0.86 kg
Mass of the largest recovered meteorite		9.83 kg
Bulk density of the meteorite		3.73
$\Gamma A'$		1.10 ± 0.04 c.g.s.
Intrinsic K		0.457 ± 0.017 c.g.s.
Initial rotation period (rotation/sec)		3.3 ± 0.3 sec
Flatness (ratio of axes of a rotational ellipsoid)		2.1 ± 0.4
Maximum head cross section height		40.7 ± 1.1 km
Drag coefficient Γ		0.7 ± 0.1
The first gross fragmentation	at a height of	40.74 ± 0.08 km
	with stripped-off mass of	59% ± 1.9%
The second gross fragmentation	at a height of	21.89 ± 0.25 km
	with stripped-off mass of	49.9% ± 2.3%
Apparent luminous efficiency τ	at 13 km s^{-1} (average)	6.1%
	at 13 km s^{-1} (one standard deviation limits)	from 3.8% to 9.7%
	at 4 km s^{-1} (average)	1.2%
	at 4 km s^{-1} (one standard deviation limits)	from 0.6% to 2.4%
Comparison of observed light curve with the computed one using apparent τ from ReVelle and Ceplecha (2001)		ε_M ±2.8 mag.[a]

[a] ε_M is the standard deviation for one measured brightness interval expressed in stellar magnitudes (the computed light curve shows large systematic deviations from the observed light curve of the same amount).

Table 2. FM solution for the Lost City bolide.

h_f (km)	Δm (%)	dt_f (sec)	dt_u (sec)	Δm_F (%)
87.9	0.008	1.2	0.2	0
86.5	0.012	1.9	0.4	0
81.8	0.030	1.9	0.55	0
77.0	0.21	2.8	1.4	0
74.0	2.3	4.9	2.4	0
60.0	0.06	2.27	2.21	0
41.0	59.5	3.25	3.24	99.96
38.0	16.0	2.11	2.10	93.5
28.0	20.0	1.61	1.60	99.99
22.0	50.0	0.71	0.70	99.99

Table 3. The Lost City bolide. Comparison of fragmentation heights and masses of fragments derived by three different methods: FM, intersection of trails, motion of the main body (dynamically derived).

FM	Intersection of trails	Dynamically derived	FM		Dynamically derived fragmentation		Dynamically derived	
Fragmentation height (km)	Separation height (km)	Fragmentation height (km)	Main mass (kg) before fragmentation	after	Main mass (kg) before fragmentation	after	Mass of large fragments[a] (kg)	
41	41.4	40.7	153	62	149	56	56	M2, a, e
38	–	–	60	50	–	–	–	–
28	30.1	–	38	30	38	26	12	M3, c, d
22	22.0	21.9	22.4	11.2	21.8	10.9	–	M4

[a] Notation of the fragments and all the dynamically derived values are those of Ceplecha (1996) with two recognized fragmentation points.

the brightness and height are compared in the corresponding figures with the observed values. Results for deceleration and mass are also compared in the corresponding figures with the dynamically derived values. Velocities derived from our FM and derived dynamically are almost identical (within the thickness of the line in Fig. 7).

FM ANALYSIS: THE INNISFREE BOLIDE

The Innisfree bolide, the maximum brightness of which can be expressed as –12 in maximum absolute panchromatic magnitude units (360–675 nm), penetrated to a height slightly below 20 km while moving along a very steep trajectory. Data from two stations of the Canadian MORP Network are available. Altogether, nine meteorites were recovered, with the largest (2.07 kg) belonging to the main trajectory.

No solution for a single gross fragmentation was found (because of many gross fragmentation points and because of K being a "strong" function of time). The single body solution follows: $\sigma = 0.0134 \pm 0.014$ s^2 km^{-2}; $\varepsilon_h = \pm 0.041$ km; ε_h is the standard deviation for one measured height; $v_1 = 14.71 \pm 0.04$ km s^{-1}. If $K = 0.58$ is assumed (average value derived from FM), the initial Innisfree mass, $m_1 = 35 \pm 9$ kg and its terminal mass $m_E = 9 \pm 3$ kg. Comparison of the observed light curve with the single body computed light curve (see Fig. 10): if the apparent τ from ReVelle and Ceplecha (2001) is used, $\varepsilon_M = \pm 3.2$ magnitudes with a systematic shift by +2.1 magnitude; if the intrinsic τ of this paper is used, $\varepsilon_M = \pm 2.2$ magnitudes with a systematic shift by –0.60 magnitudes, where ε_M is the standard deviation for one measured brightness interval in units of panchromatic stellar magnitudes. The single body solution is not able to explain the light curve at all. These single body Innisfree mass values are also similar to those deduced by ReVelle (1979) whose analysis did not formally include fragmentation effects. Similar comments also apply to the Lost City bolide entry analysis by ReVelle (1979) as well.

However, the FM solution yielded the following results. The shape density coefficient K was large during the early part of the trajectory, and subsequently decreased to ~0.5. Ablation of large fragments was not at all significant for the observed light curve. This was also recognized "observationally" in the original paper on Innisfree (Halliday et al. 1981), where the caption for Fig. 4 reads: "The fragments separated from the main mass at various times, but their contribution to the total luminosity is a minor one until the very last stages." If fragment "B" is dealt with as the main mass below 32 km height, this statement holds actually for the entire trajectory. In any case, fragmentation into large pieces for Innisfree was not found to be necessary at all in order to provide an explanation of its light curve. Compared to the results on the Lost City bolide, the situation for Innisfree is very different. The solution for Lost City required much smaller values of σ than the average value of 0.014 s^2 km^{-2} that has been determined previously to be that of a typical type I chondritic meteorite. The starting value of $\sigma = 0.008$ s^2 km^{-2} decreases to a value of 0.004 s^2 km^{-2} at heights below 26 km. The resulting initial mass of 42 kg is about twice as large as that given by Halliday et al. (1981); it is actually on the upper edge of the derived range of their possible initial masses. The terminal mass computed from our FM is 2.03 kg compared to 2.07 kg of the largest recovered meteorite belonging to trail "B." The computed single body terminal masses are also significantly larger.

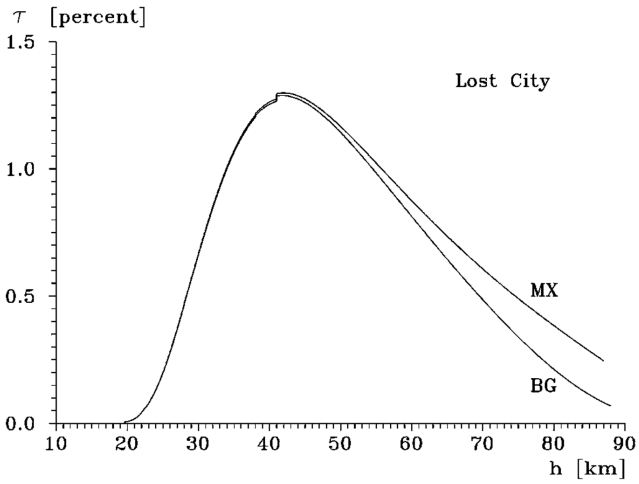

Fig. 1. Intrinsic luminous efficiency τ as function of height for the Lost City bolide: MX = with normalizing the intrinsic τ by the height of maximum light; BG = with normalizing the intrinsic τ by the beginning height.

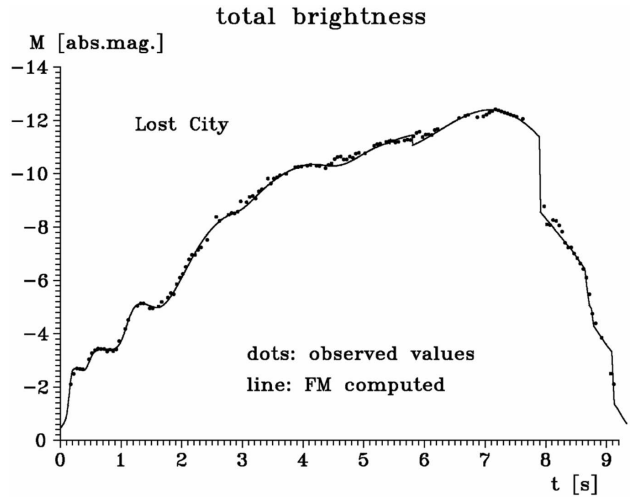

Fig. 2. Comparison of the FM computed and observed total brightness of the Lost City bolide.

With the following values, we were able to fully explain the dynamics (height as function of time) and light production for the Innisfree bolide. The fit shows a systematic shift at the two last points before the termination of the light. Without these two points, the fit yields $\sigma = 0.008$–0.004 s^2 km^{-2}; $\varepsilon_h = \pm 0.025$ km; ε_h is the standard deviation for one measurement of height; $K = 0.25$–0.96 in c.g.s. units; (σ and K are functions of time;

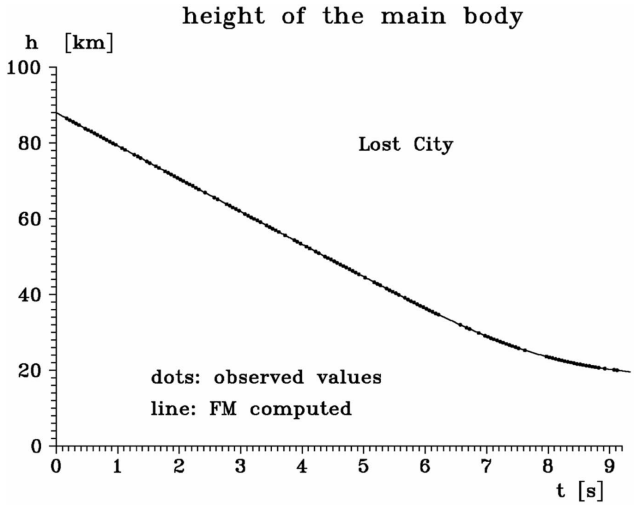

Fig. 3. Comparison of the FM computed and observed height of the Lost City bolide.

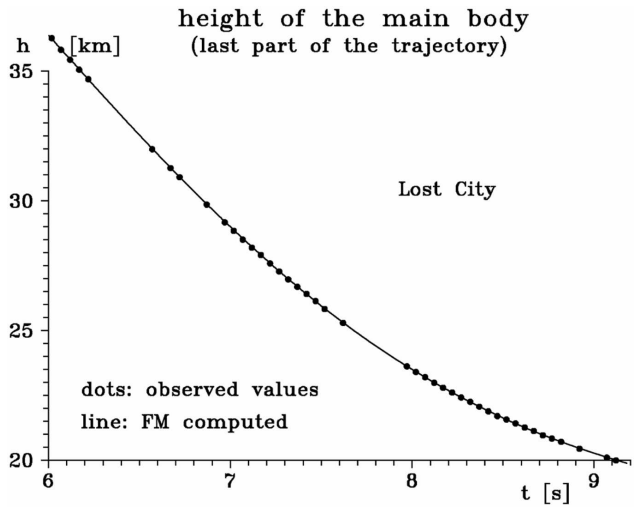

Fig. 4. Comparison of the FM computed and observed height during the last part of the Lost City bolide trajectory.

see their derived behavior in Figs. 18 and 19); v_1 = 14.698 ± 0.035 km s^{-1}; m_1 = 42 ± 2 kg; ε_M = ±0.14 magnitudes (intrinsic τ used); ε_M is the standard deviation for one measurement of brightness also expressed in terms of stellar magnitudes. The resulting σ and K are also given in Table 4. (For an explanation of the symbols see the Lost City solutions). Our FM fits the observed height as a function of time and the light curve data within the precision of the observations. No significant discrepancies remain outside of the computed standard deviations, except for the brightness at the last two points. The latter effect may also be caused by variations of the luminous efficiency parameter at extremely low velocities. The results of the FM are also compared to the single body solutions in Figs. 10–20.

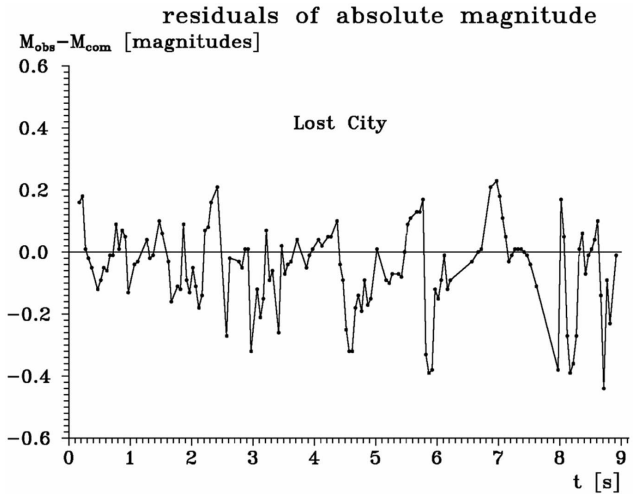

Fig. 5. Residuals of magnitudes of the FM fit to the light curve of the Lost City bolide.

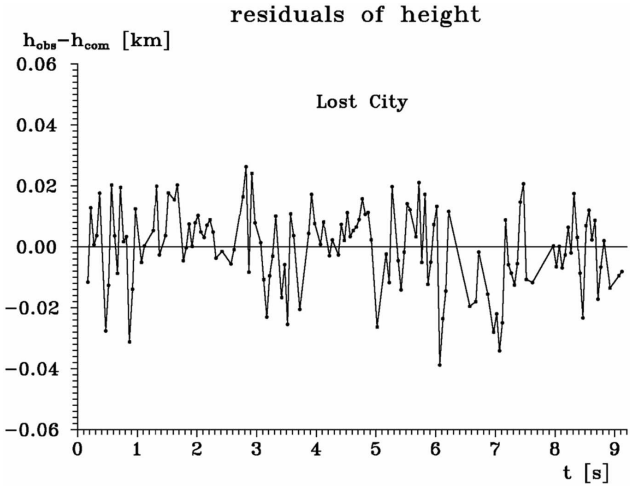

Fig. 6. Residuals of heights of the FM fit to the observed height as function of time of the Lost City bolide.

FM ANALYSIS: THE BENEŠOV BOLIDE

The Benešov bolide, which attained a maximum absolute panchromatic stellar magnitude of almost –20, penetrated to a height of 17 km (with good data existing down to 19.8 km). Data from four Czech stations of the European Fireball Network are available. Moreover, two grating spectra were also recorded at the Ondřejov Observatory (Spurný 1994; Borovička and Spurný 1996). Stony composition is evident and a fall of several small meteorites is almost certain, however, no meteorites were recovered after a thorough search. There is direct evidence of meteoroid fragmentation at altitudes of 38–31 km (discernible trails of nine individual fragments were photographed) and of a catastrophic disruption at the height of 24 km.

No solution was found for a single gross fragmentation

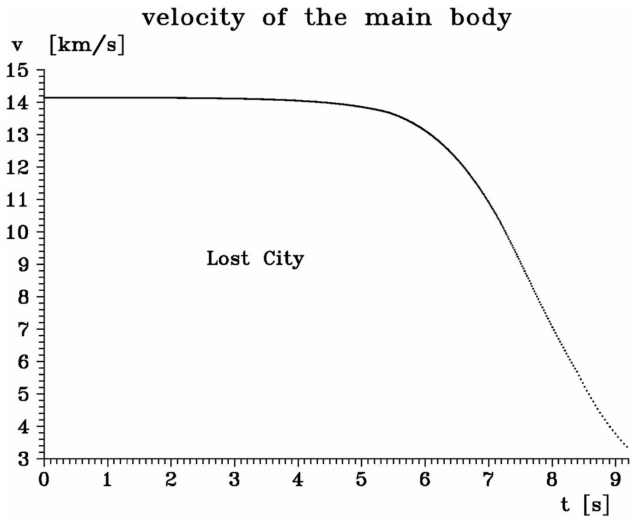

Fig. 7. The FM computed velocity of the Lost City meteoroid. Dynamical solution with 2 recognized fragmentation points (Ceplecha 1996) is almost identical to the FM solution (inside thickness of the line).

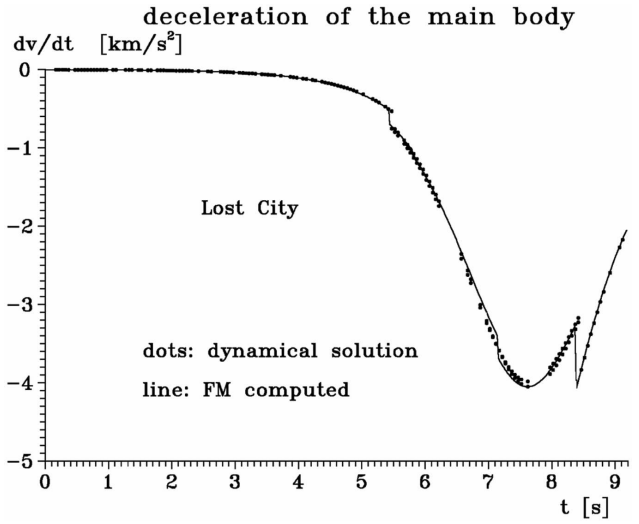

Fig. 8. The FM computed deceleration of the Lost City meteoroid. The dots correspond to the dynamical solution with two recognized fragmentation points (Ceplecha 1966).

event (because of many gross fragmentation points and because of K being a very "strong" and "peaked" function of time). The deduced single body solution follows: $\sigma = 0.0135 \pm 0.004$ s^2 km^{-2}; the standard deviation for one measurement of height, $\varepsilon_h = \pm 0.047$ km; $v_1 = 21.326 \pm 0.009$ km s^{-1}; bolide type I; $m_1 = 75 \pm 6$ kg. Comparison of the observed light curve with the single body computed light curve: if the apparent τ from ReVelle and Ceplecha (2001) is used, $\varepsilon_M = \pm 2.5$ magnitudes; if the intrinsic τ of this paper is used, $\varepsilon_M = \pm 4.4$ magnitudes with a systematic shift by 3.5 magnitudes, where ε_M is the standard deviation for one measured brightness interval in stellar magnitudes. Again, the single body solution is not able to explain the light curve.

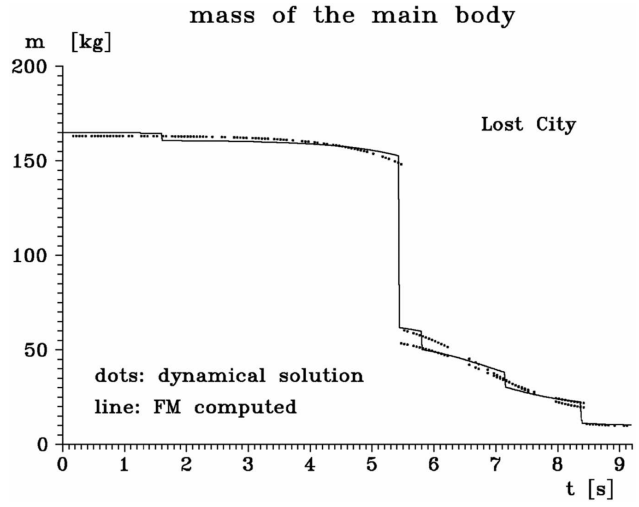

Fig. 9. The FM computed mass of the Lost City bolide. The dots correspond to the dynamical solution with two recognized fragmentation points (Ceplecha 1966).

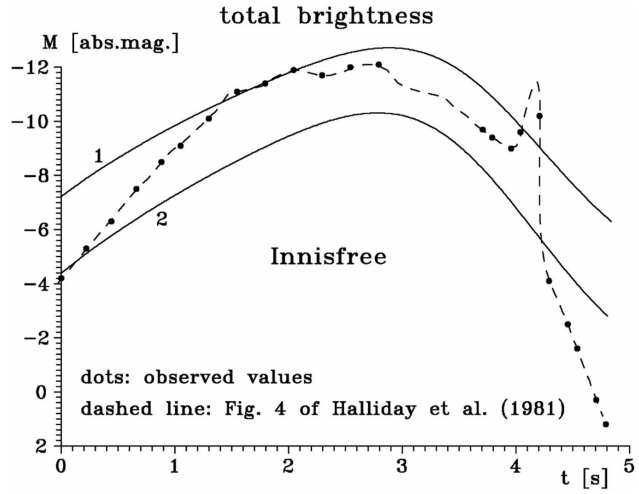

Fig. 10. Observed and single body computed total brightness of the Innisfree bolide; 1 = single body solution with apparent τ (ReVelle and Ceplecha 2001); 2 = single body solution with intrinsic τ.

Applying our FM to the Benešov bolide data, the shape density coefficient was found to be quite anomalous. The resulting K has a very small value at the beginning of the trajectory. It then changes to extremely large values during the central parts of the trajectory and changes again to small values near the end of the trajectory. This behavior may have been caused by large fragments being less important for the light curve above 70 km and also below 45 km. The FM solution also required lower values of σ than is the average for typical type I bolides. The resulting initial mass of 4100 kg is much larger than the "dynamical value" computed from the single body solution (75 kg) and also smaller than the originally estimated "photometric mass" (15,000 kg: Spurný 1994), and about twice the value resulting from radiative hydrodynamic modeling (2000 kg) given in Borovička et al. (1998).

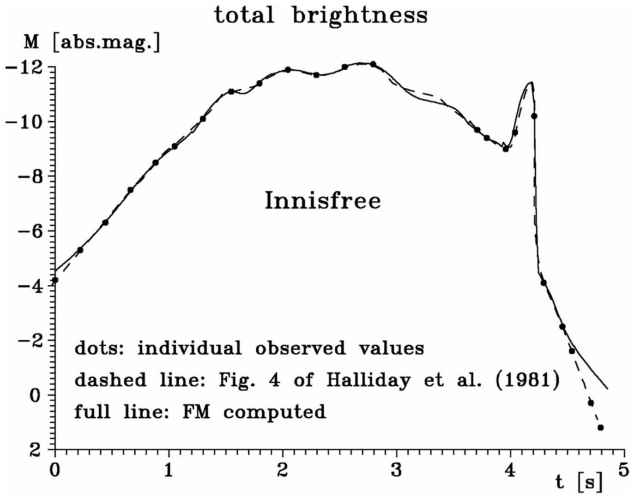

Fig. 11. Comparison of the FM computed and observed total brightness of the Innisfree bolide.

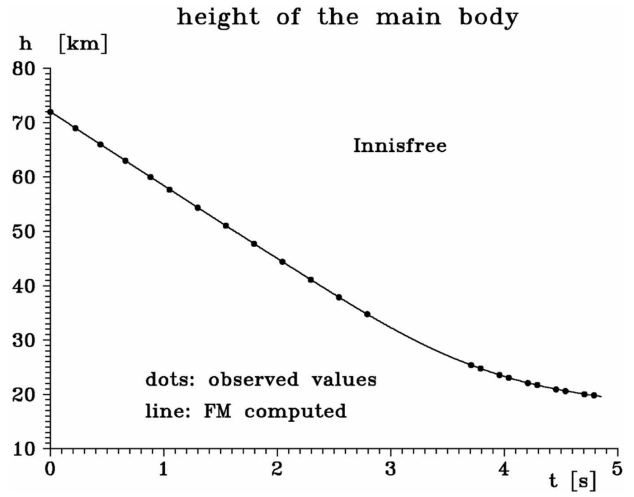

Fig. 12. Comparison of the FM computed and observed height of the Innisfree bolide.

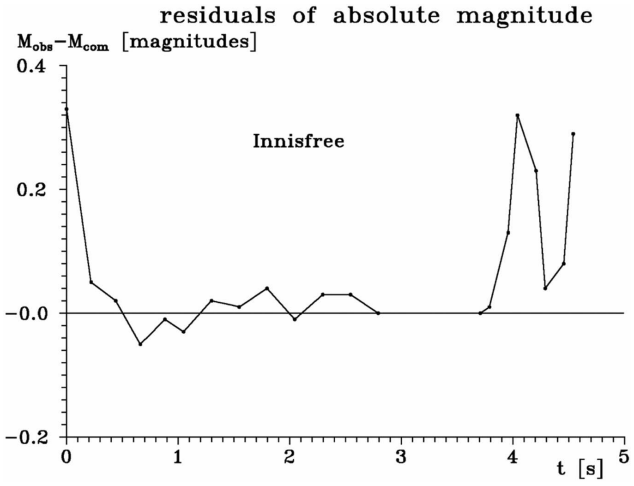

Fig. 13. Residuals of magnitudes of the FM fit to the light curve of the Innisfree bolide

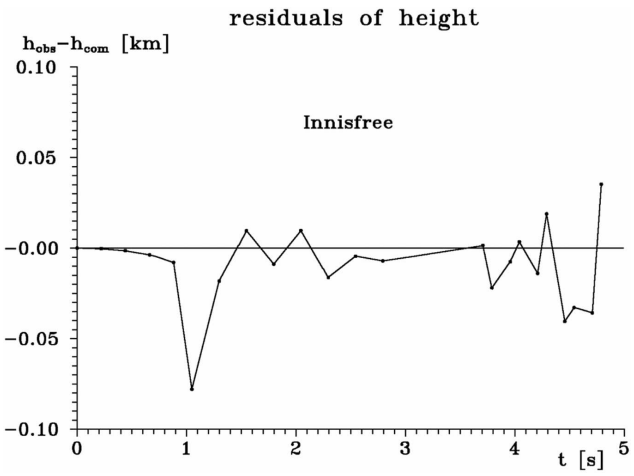

Fig. 14. Residuals of heights of the FM fit to the observed height as function of time of the Innisfree bolide.

However, applying our FM to observational data on the Benešov bolide, the following values resulted. They fully explain the dynamics (height as function of time) and light curve of the Benešov bolide: $\sigma = 0.008–0.005$ s^2 km^{-2}; the standard deviation for one measurement of height, $\varepsilon_h = \pm 0.046$ km; $K = 0.023–2.2$ in c.g.s. units; σ and K are functions of time: see Figs. 29 and 30; $v_1 = 21.317 \pm 0.012$ km s^{-1}; $m_1 = 4100 \pm 100$ kg; the standard deviation for one measured brightness interval, $\varepsilon_M = \pm 0.19$ stellar magnitudes. The resulting σ and K are also indicated in Table 5. (For explanations of the symbols: see the Lost City solutions.) The results are given in Figs. 21–31 and compared to the single body solution (denoted as the "dynamical solution" in the graphs). Our FM fits the height as function of time and the light curve of the Benešov bolide within the precision of the observations. Compromising the two independent fits, i.e., the light curve fit and the height-as-function-of-time fit, resulted in small, partly periodic and systematic changes of residuals in the deduced heights (Fig. 25). In Table 6, we compare the fragmentation heights derived from our FM with the separation heights observed, i.e., heights derived from the intersection of individually observed trails of different fragments with the trail of the main body as published by Borovička et al. (1998). The two sets of fragmentation heights in Table 6 are completely independent values. The FM fragmentation heights were derived from our FM, i.e., from a simultaneous FM fit to the observed height as function of time and to the observed light curve (both for the main body), whereas the separation heights were determined by the intersection of individually observed trails of large fragments with the trail of the main body. In principle, large fragments could have been separated from the main body at different heights than the FM fragmentation heights, where release of a large number of small fragments is assumed in the model. However, Table 6 points to the separation of large fragments

Table 4. FM solution for the Innisfree bolide.

h_f (km)	Δm (%)	dt_f (sec)	dt_u (sec)	K (c.g.s.)	σ ($s^2\,km^{-2}$)
71.8	2.0	2.1	1.3	0.96	0.008
58.1	3.8	1.0	0.5	0.86	0.008
55.6	30	2.2	0.8	0.46	0.008
46.2	42	2.0	0.85	0.27	0.008
41	–	–	–	0.25	0.008
38	–	–	–	0.65	0.008
36	20	1.5	0.8	0.60	0.008
34.7	11	1.5	1.1	0.48	0.008
26	6	0.8	0.4	0.35	0.006
23.72	61	0.32	0.26	0.38	0.004
23.2	1.5	0.8	0.25	0.38	0.004

Table 5. FM solution for the Benešov bolide.

h_f (km)	Δm (%)	dt_f (sec)	dt_u (sec)	K (c.g.s.)	Δm_F (%)	σ ($s^2\,km^{-2}$)
90.4	0.016	1.2	0.50	0.023	0	0.008
80.2	0.001	1.0	0.35	0.07	0	0.008
77.4	0.0007	0.28	0.17	0.16	0	0.008
70.1	0.05	1.0	0.20	0.23	0	0.008
66.1	0.6	1.0	0.28	0.52	65	0.007
66.0	3.6	1.1	0.62	0.52	80	0.007
55.7	0.1	0.8	0.4	1.2	0	0.007
51.5	0.001	1.0	0.2	1.6	0	0.006
45.3	3.0	0.7	0.26	2.2	0	0.006
39.8	14	0.46	0.28	2.0	0	0.005
36.1	38	0.70	0.3	1.8	0	0.005
29.5	19	0.40	0.20	1.1	0	0.005
25.9	83	0.21	0.16	0.84	0	0.005
24.3	97	0.55	0.10	0.43	0	0.005

Table 6. The Benešov bolide: comparison of fragmentation heights derived from FM and from intersection of trails. For the notation of fragments see Borovička et al. (1998).

FM fragmentation height (km)	Separation height (km)	Fragment #
45.3	42	8
39.8, 36.1	37.5	1, 2
29.5	27	5
25.9, 24.3	24.2, 23.5	7, 6

at approximately the same heights, where also a large number of tiny particles was released and overwhelmingly contributed to Benešov bolide radiation. This is very different from the Lost City bolide, where radiation of individual large fragments was relatively more important compared to the radiation of small fragment clusters.

The terminal mass of the main body of Benešov was found to be 2.7 kg. However, large fragments are certainly hidden in the overwhelming radiation originating from clusters of small fragments. Information on these larger fragments are available only from the study of Borovička et al. (1998), who analyzed very large fragments from their individually discernible trails

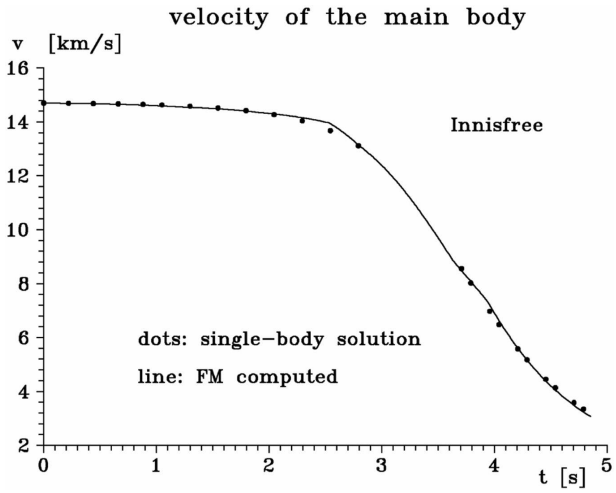

Fig. 15. The FM computed velocity of the main body of the Innisfree bolide is compared to the single body solution.

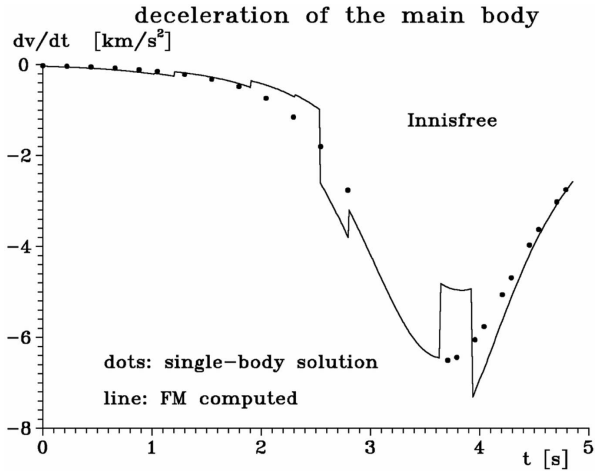

Fig. 16. The FM computed deceleration of the main body of the Innisfree bolide is compared to the single body solution.

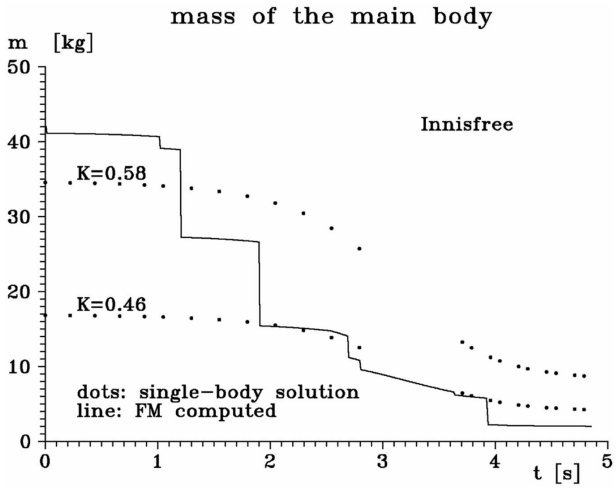

Fig. 17. The FM computed mass of the main body of the Innisfree bolide is compared to the single body solution with two different K.

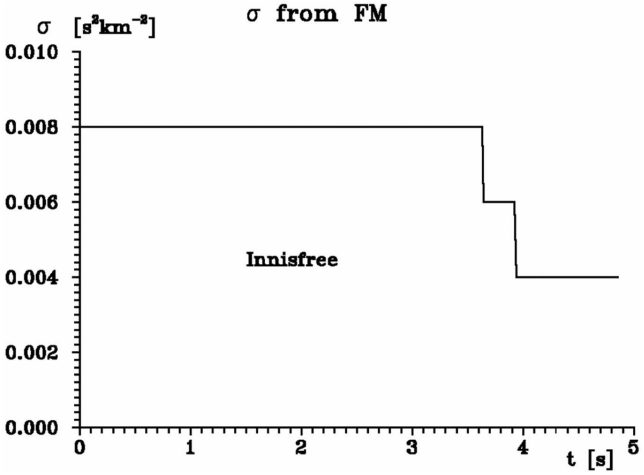

Fig. 18. The intrinsic ablation coefficient of the Innisfree meteoroid derived from the FM fit to observation.

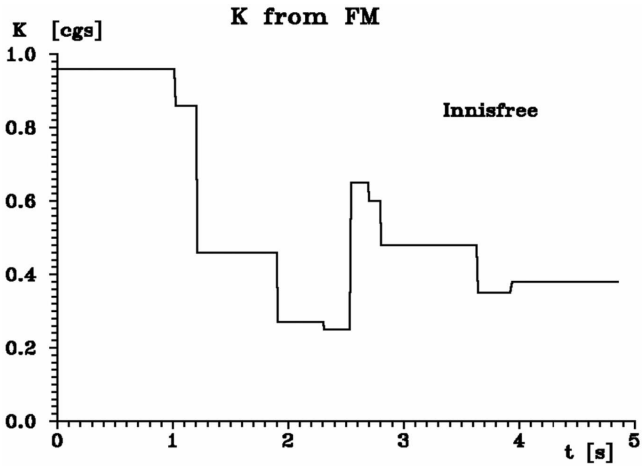

Fig. 19. The shape density coefficient *K* of the Innisfree meteoroid derived from the FM fit to observation.

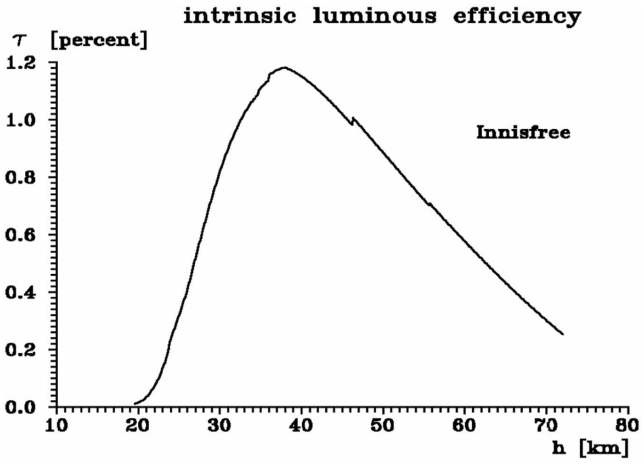

Fig. 20. The intrinsic luminous efficiency of the Innisfree meteoroid corresponding to the FM fit to observation.

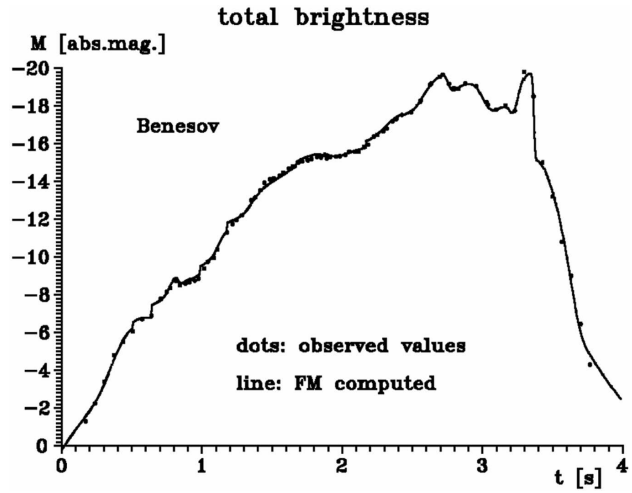

Fig. 21. Comparison of the FM computed and observed total brightness of the Benešov bolide.

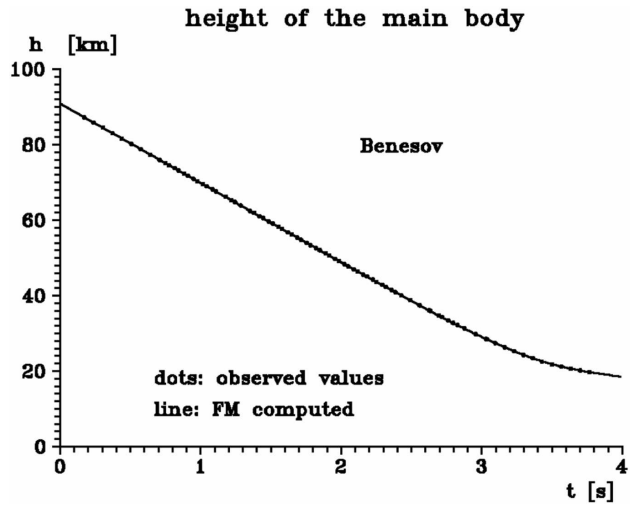

Fig. 22. Comparison of the FM computed and observed height of the Benešov bolide.

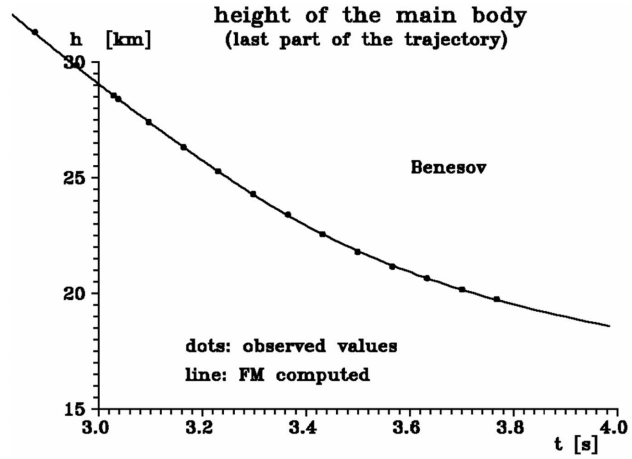

Fig. 23. Comparison of the FM computed and observed height during the last part of the Benešov bolide trajectory.

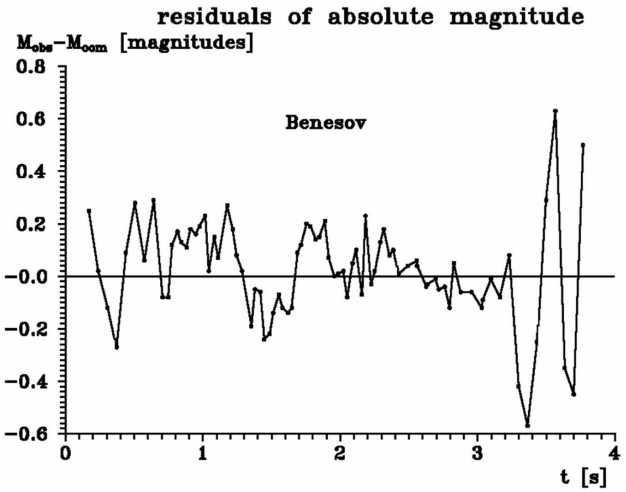

Fig. 24. Residuals of magnitudes of the FM fit to the light curve of the Benešov bolide.

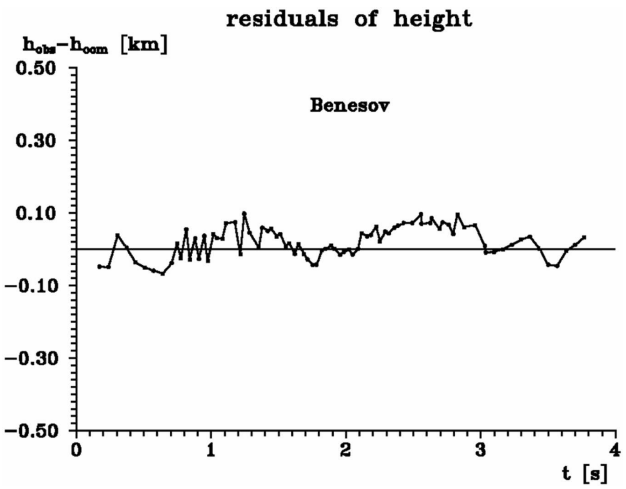

Fig. 25. Residuals of heights of the FM fit to the observed height as function of time of the Benešov bolide.

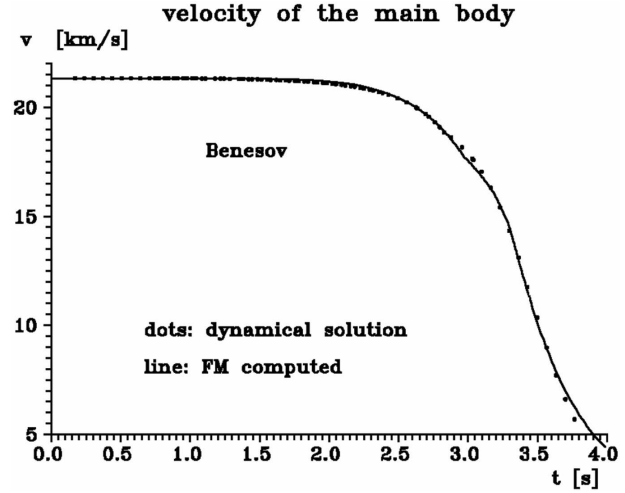

Fig. 26. The FM computed velocity of the main body of the Benešov bolide is compared to the single body solution (dynamical solution).

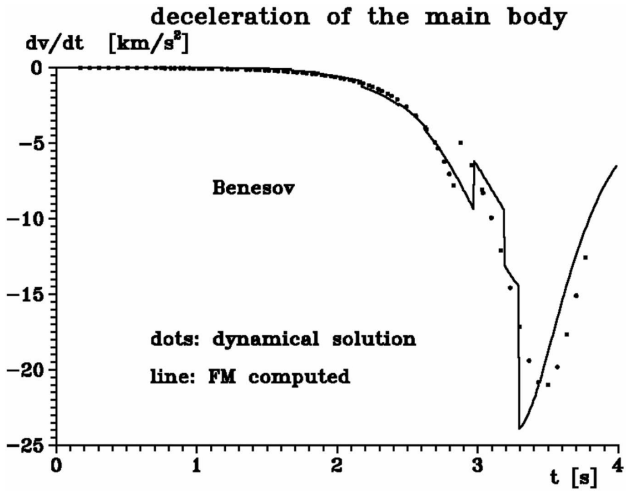

Fig. 27. The FM computed deceleration of the main Benešov bolide body is compared to the single body solution (dynamical solution).

on the original photographs. This also points to a natural limitation of modeling of the main body motion and radiation by using only data on the main body trajectory. Analysis of the Benešov bolide by our FM proved that the concept of the intrinsic τ significantly improves the results. No significant discrepancies remain outside the computed standard deviations. The small systematic changes of residua with time originate perhaps from fitting too many parameters with grossly different influences on either the height as function of time or on the light curve.

Upon request of our reviewer, we present also coordinates of possible meteorite impacts belonging to the Benešov bolide. Spurný (2004, personal communication) derived them and kindly authorized us to publish his results in our paper. Due to a very steep trajectory, all fragments should have landed close to the main mass of several kilograms at 49.777°N and 14.614°E (coordinate system S42). In a vicinity of several hundred meters around this location, all pieces belonging to trajectories in Borovička et al. (1998; Fig. 6) should have landed.

SURVEY OF FM ANALYSIS APPLIED TO 15 BOLIDES

We applied our FM model to a total of 15 bolides. All fits were successful and we were able to reproduce the observed height as function of time and the observed light curve for all 15 of them with a precision corresponding to the precision of the observations. Our choice of events includes different types of bolides with very different velocities and brightness levels. We also applied the FM to bright Leonids with very high altitude radiation (with measurements as high as 200 km in height). We were able to explain the anomalous high altitude radiation of Leonids together with the change into

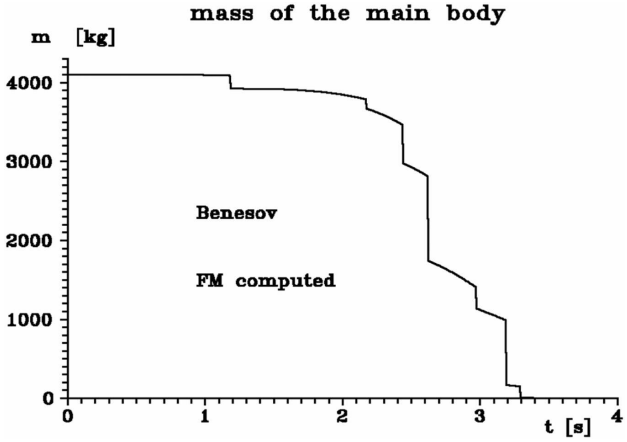

Fig. 28. The FM computed mass of the main body of the Benešov bolide. The dynamically derived mass (the single body solution) is not contained in this figure because it is extremely and unrealistically low (starts with 75 kg).

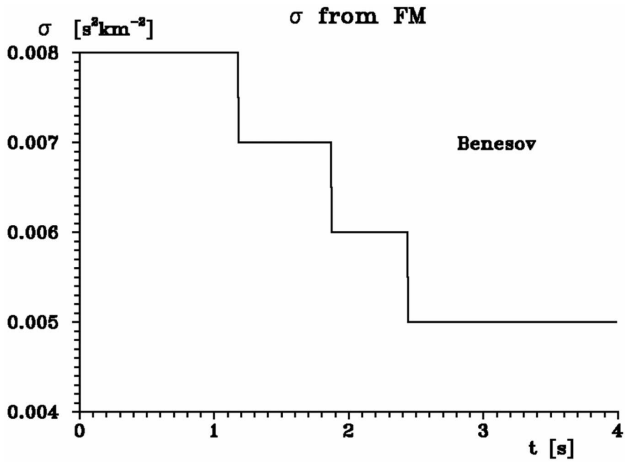

Fig. 29. The intrinsic ablation coefficient of the Benešov meteoroid derived from the FM fit to observation.

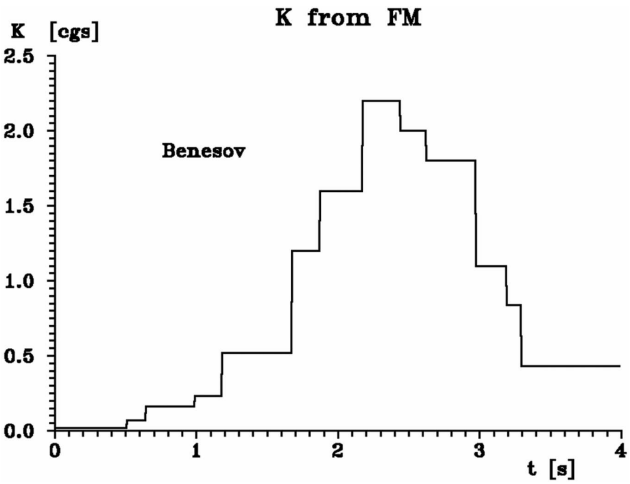

Fig. 30. The shape density coefficient *K* of the Innisfree meteoroid derived from the FM fit to observation.

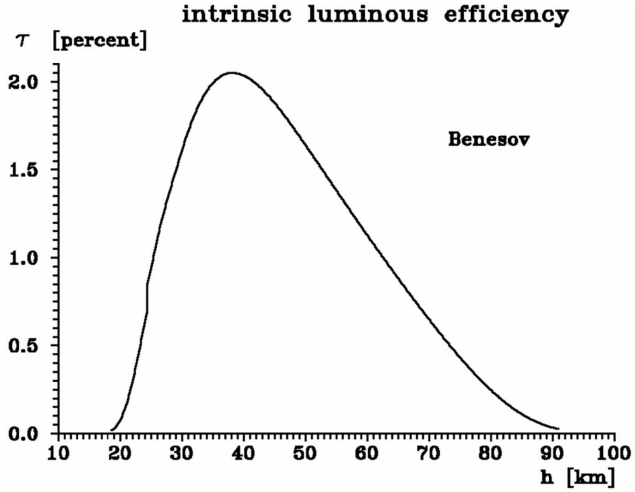

Fig. 31. The intrinsic luminous efficiency of the Innisfree meteoroid corresponding to the FM fit to observation.

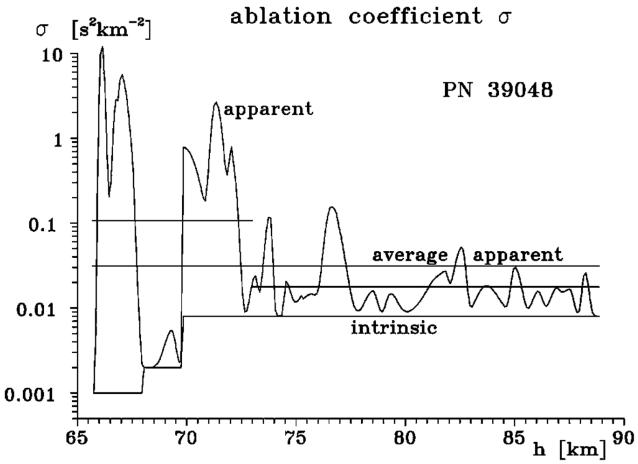

Fig. 32. Comparison of the intrinsic (the FM derived) and the apparent ablation coefficient of the PN 39048 bolide.

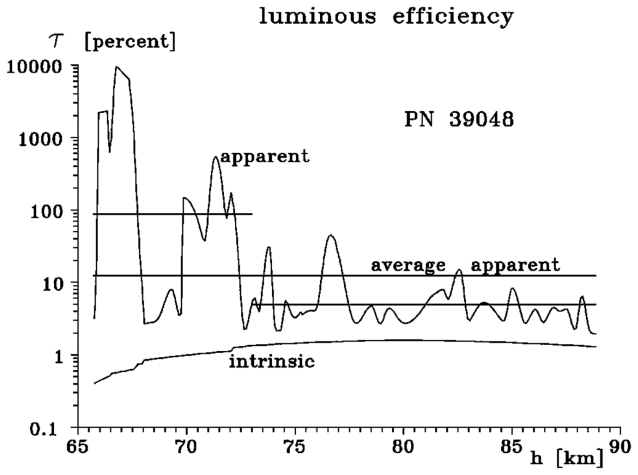

Fig. 33. Comparison of the intrinsic (corresponding to the FM fit) and the apparent luminous efficiency of the PN 39048 bolide.

Table 7. Survey of results of the FM fit to 15 bolides.[a]

Bolide nr.	Lost City	Innisfree	PN 39048	PN 39093B	PN 39337A	PN 40503	EN 250203	EN 270200
Type	I	I	IIIB	II–IIIA	IIIA	II	I	I
h_1 km	86.5	72.0	88.5	69.5	96.9	92.7	74.1	80.1
h_E km	19.9	19.8	66.1	42.5	75.6	21.9	33.9	31.6
v_1 km s^{-1}	14.1486	14.698	22.151	18.298	38.547	20.830	13.925	18.79
	±0.0014	±0.035	±0.010	±0.011	±0.012	±0.012	±0.002	±0.012
z_1	51.88°	22.06°	70.4°	18.32°	79.01°	51.53°	61.90°	16.96°
M_{max} magnitude	–12.4	–12.1	–12.6	–12.3	–14.0	–20.0	–7.1	–10.1
h_{max} km	27.9	34.7	67.1	54.9	80.6	22.3	45.7	46.5
m_1 kg	165	42	1.50	4.8	0.56	1100	1.80	3.6
	±6	±2	±0.15	±0.2	±0.06	±80	±0.07	±0.2
σ s^2 km^{-2}	0.008	0.004–0.008	0.001–0.008	0.004–0.009	0.004–0.012	0.001–0.004	0.004–0.008	0.004
K c.g.s.	0.46	0.25–0.96	1.4–4.0	0.45–1.45	0.6–1.9	0.02–1.0	0.36–1.02	0.12–1.65
τ%	0.01–1.29	0.01–1.18	0.6–1.6	0.30–0.55	0.5–2.4	0.01–1.98	0.01–1.03	0.01–1.52
ε_h km	±0.013	±0.025	±0.018	±0.018	±0.009	±0.067	±0.007	±0.018
ε_M magnitude	±0.17	±0.14	±0.12	±0.13	±0.06	±0.07	±0.26	±0.11
n_A, n_B, n_C, n_D	1, 0, 2, 2	2, 2, 3, 2	1, 2, 1, 5	1, 0, 1, 5	1, 3, 2, 2	1, 1, 2, 2	1, 1, 1, 0	0, 3, 2, 2
Bolide nr.	Benešov	LN 98002	LN 98011	LN 98023	LN 98043	EN 120801	EN 020602	
Type	I	IIIA	IIIA	IIIA	IIIA	IIIA	I	
h_1 km	87.3	150.2	185.7	199.4	178.2	145.1	83.9	
h_E km	19.8	103.0	95.3	73.3	87.6	79.2	27.7	
v_1 km s^{-1}	21.317	72.41	72.68	72.82	71.64	58.21	16.746	
	±0.012	±0.04	±0.11	±0.13	±0.06	±0.27	±0.006	
z_1	9.30°	75.85°	59.38°	42.63°	21.78°	49.19°	27.26°	
M_{max} magnitude	–19.8	–7.6	–7.6	–12.2	–6.7	–7.9	–11.1	
h_{max} km	24.3	104.8	100.9	84.4	92.8	81.6	42.9	
m_1 kg	4100	0.008	0.017	0.55	0.0012	0.010	2.2	
	±100	±0.001	±0.002	±0.12	±0.0004	±0.002	±0.2	
σ s^2 km^{-2}	0.005–0.008	0.0013–0.0075	0.004–0.008	0.002–0.014	0.005–0.011	0.004–0.015	0.001–0.002	
K c.g.s.	0.023–2.2	0.6–1.4	0.6–0.9	0.3–2.5	0.6–1.2	0.35–1.10	0.1–0.8	
τ%	0.06–2.05	1.49–3.31	0.66–3.38	0.02–4.48	0.27–3.24	0.17–2.67	0.02–1.24	
ε_h km	±0.046	±0.019	±0.089	±0.062	±0.053	±0.020	±0.036	
ε_M magnitude	±0.19	±0.05	±0.07	±0.07	±0.06	±0.06	±0.32	
n_A, n_B, n_C, n_D	1, 1, 2, 3	2, 4, 4, 2	4, 3, 2, 0	0, 2, 2, 2	0, 4, 2, 1	0, 2, 3, 1	1, 0, 0, 1	

[a] h_1 = beginning height; h_E = terminal height; v_1 = velocity at the beginning height with its standard deviation; z_1 = inclination of the trajectory to vertical line at the beginning; M_{max} = maximum absolute magnitude (distance of 100 km); h_{max} = height of the maximum light; m_1 = mass of the body at the beginning height; σ = intrinsic ablation coefficient; K = shape density coefficient; τ = intrinsic luminous efficiency; ε_h = standard deviation of the FM fit to the observed height curve (height as function of time) for one measured height; ε_M = standard deviation of the FM fit to the observed light curve for one measured brightness; n_A, n_B, n_C, n_D = number of fragmentation events between 1 to 3, 3 to 10, 10 to 30, 30 to 100% of the main body, respectively.

"normal" radiation after the "normal" ablation started (Spurný et al. 2000a, b). It would be impractical to publish the results the same detailed way as we did for the Lost City, Innisfree, and Benešov bolides. Thus, we only summarized the most important results in Table 7. Following advice of our reviewer, we intend to publish more details on Leonids in a separate paper.

RECOMPUTED APPARENT VALUES OF σ AND τ

Following the definition of the apparent and the intrinsic values of the ablation coefficient σ and the differential luminous efficiency τ and having performed the FM solution for any bolide event, we recomputed the apparent values of σ and τ from their intrinsic values. While all values of σ and τ derived in the past were apparent values, it might be important to derive some sort of comparison between these two sets of quantities. In fact, we have already done this for all 15 bolides that we solved by fitting their observed data to our FM. We found that the apparent values of σ and τ change during the bolide trajectory substantially and, moreover, are much larger than their intrinsic values. This difference increases with the bolide type as we progress toward bodies of progressively higher end height (with all bodies having the same value of mass, velocity, entry angle, etc.). For type IIIA and IIIB bolides, the apparent luminous efficiency values are unrealistic and of the order of 100% over at least part of the trajectory. There is not much realism in computing average values of the recomputed apparent σ and τ because they span over several orders of magnitude. Hence, we can see that

using a single apparent value of σ or τ for one bolide event will yield quite unrealistic results. Using the apparent values of σ and τ was based on an incorrect assumption that fragmentation processes had a negligible or small influence on the bolide motion and light emission, while just the opposite turns out to be the normal case, i.e., fragmentation is the primary process of large (and perhaps small) meteoroid ablation. The light curve represents the radiation of the main body and the large fragments and the clusters of small fragments, while the change of height with time (dynamics of the main body) represents only that of the main body itself.

As an example, we present the recomputed apparent values of σ and τ for a IIIB bolide PN 39048 in Figs. 32 and 33. While the intrinsic values of σ are within an interval of 0.001–0.008 $s^2\,km^{-2}$, the apparent values of σ are larger and strongly oscillate up to values over 10 $s^2\,km^{-2}$. The averages of the logarithmic values presented in Fig. 32 do not have much meaning due to differences of actual values by several orders, but the terminal part corresponds to apparent σ values mostly over 0.1 $s^2\,km^{-2}$, while the previously deduced average value of the apparent σ for IIIB type is 0.2 $s^2\,km^{-2}$. The values of the apparent τ in Fig. 33 oscillate similarly as for σ. An "average" value for the whole trajectory is 10% and for the terminal part of the trajectory it is 100%. Individual values of the apparent τ are almost 10,000%. All these unrealistic apparent values just reflect the fact that the fragmentation process was neglected. Fragmentation into big fragments and clusters of small fragments is the main process of mass loss of meteoroids. Results of the recomputed apparent values of σ and τ for all studied bolides are similar to those presented in Figs. 32 and 33 and the differences between the intrinsic and apparent values of σ and τ are systematically smaller for bolides with progressively lower end heights ("lower type") (with all bodies having the same value of mass, velocity, entry angle, etc., i.e., from type IIIB to type I).

Our FM fully explains a well-known dilemma of meteor physics. Meteoroid masses derived only from meteor light emission are larger by orders of magnitude than meteoroid masses derived from meteoroid motion (difference of "photometric" and "dynamic" masses). The dilemma is evidently caused by not accounting properly for fragmentation. "Photometric" masses are more influenced by fragmentation than are the "dynamic" masses. However, fragmentation into several large fragments may also significantly change the resulting "dynamic" mass. The FM properly accounts for fragmentation and yields just one value of mass at each trajectory point—the realistic value of mass of the main body of a meteoroid.

CONCLUSIONS

1. The fragmentation model (FM) presented in this paper was successfully applied to 15 bolides of different types, masses, and velocities, and has been found to perform nearly flawlessly, i.e., the two independent fits of height as function of time and of the light curve correspond to standard deviations of the observations on good quality observational data for bolides of all types, including very high altitude radiation of extremely fast meteoroids.
2. The intrinsic and apparent values of the ablation coefficient σ and of the luminous efficiency τ were both examined for the first time. Introducing the new concepts of the intrinsic and apparent values of the luminous efficiency τ and of the ablation coefficient σ has produced a breakthrough in our understanding of bolides and their dynamical and luminous behavior.
3. Values of the intrinsic ablation coefficient σ are very small, independent of the previously defined bolide types, mass, velocity, or even of height of penetration. They are mostly lower than even the type I apparent values of σ, occupying a rather narrow interval between 0.001 and 0.015 $s^2\,km^{-2}$, with the most typical values being about 0.004–0.008 $s^2\,km^{-2}$. Large values of the apparent ablation coefficient increasing from type I (σ = 0.014 $s^2\,km^{-2}$) to type IIIB (σ = 0.21 $s^2\,km^{-2}$) reflect primarily the processes of fragmentation. The fragmentation process cannot be modeled solely by utilizing larger values of the apparent ablation coefficient, but needs to be formally incorporated into models that can go beyond the simple single body modeling limit (see also ReVelle 2002).
4. Purely theoretical models assuming inhomogeneous bodies with a different percentage of porosity (ReVelle 2001) reflect this situation better than the classical single body theory or the gross fragmentation model (Ceplecha 1993).
5. Introducing intrinsic values of σ and τ, the FM fully explains a long-lasting dilemma of meteor physics: meteor masses derived from meteor light were larger than meteor masses derived from meteor motion by as many as several orders of magnitude (the so-called difference of the "photometric" mass computed from meteor luminosity and the "dynamic" mass computed from meteor body change of motion). This dilemma was evidently caused by not accounting properly for the fragmentation process and by using apparent values of σ and τ. Most of the light from type IIIA- and type IIIB-bolides originates from fragments that have already been liberated, and not directly from the main body itself.
6. The fragmentation process cannot even be simply modeled by the sole introduction of just very large values of the apparent luminous efficiency. Before we invented our FM and performed our FM modeling with the intrinsic values of the luminous efficiencies, an explanation of these extremely large values of the "observed" luminous efficiencies was completely absent.
7. Our model works not only in the range of "classical" meteor radiation below heights of ~130 km, but also for

recently revealed radiation of very fast bodies at very high elevations up to 200 km (Spurný et al. 2000a, b).

8. The derived values of the shape density coefficient roughly correspond to average values that were published previously for each corresponding bolide type (Table XVII in Ceplecha et al. 1998). It would be interesting to compute "absolute" densities of meteoroids, but without exact values of the drag coefficient Γ itself as a function of shape, rotation effects, Mach number, and Reynolds number, etc., this is simply not possible.

Editorial Handling—Dr. Donald Brownlee

REFERENCES

Adolfson L. Forthcoming. Rotation of meteors: Lost City. *Icarus.*

Ayers W. G., McCrosky R. E., and Shao C. Y. 1970. Photographic observations of 10 artificial meteors. Special Report 317. *Smithsonian Astrophysical Observatory Contributions to Astrophysics.* pp. 1–40.

Babadzanov P. B. 1991. Fragmentation and densities of meteoroids. Proceedings, Asteroids, Comets, Meteors 1991 Conference. Houston: Lunar and Planetary Institute. pp. 23–26.

Borovička J. and Spurný P. 1996. Radiation study of two very bright terrestrial bolides. *Icarus* 121:484–510.

Borovička J., Popova O. P., Nemtchinov I. V., Spurný P., and Ceplecha Z. 1998. Bolides produced by impact of large meteoroids into the Earth's atmosphere: Comparison of theory with observations. I. The Benešov bolide dynamics and fragmentation. *Astronomy and Astrophysics* 334:713–728.

Ceplecha Z. 1996. Luminous efficiency based on photographic observations of the Lost City fireball and implications for the influx of interplanetary bodies onto Earth. *Astronomy and Astrophysics* 311:329–332.

Ceplecha Z. 1988. Earth's influx of different populations of sporadic meteoroids from photographic and television data. *Bulletin of the Astronomical Institutes of Czechoslovakia* 39:221–236.

Ceplecha Z., Spurný P., Borovička J., and Keclíková J. 1993. Atmospheric fragmentation of meteoroids. *Astronomy and Astrophysics* 279:615–626.

Ceplecha Z., Borovička J., Elford W. G., ReVelle D. O., Hawkes R. L., Porubcan V., and Šimek M. 1998. Meteor phenomena and bodies. *Space Science Reviews* 84:327–471.

Halliday I., Blackwell A. T., and Griffin A. A. 1978. The Innisfree meteorite and the Canadian camera network. *Journal of the Royal Astronomical Society of Canada* 72:15–39.

Halliday I., Griffin A. A., and Blackwell A. T. 1981. The Innisfree meteorite fall: A photographic analysis of fragmentation, dynamics, and luminosity. *Meteoritics* 16:153–170.

Öpik E. J. 1933. Atomic collisions and radiation of meteors. *Acta et Commentationes Universitatis Tartuensis* 26:1–39.

Öpik E. J. 1955. Meteor radiation, ionization, and atomic luminous efficiency. *Proceedings of the Royal Society of London. Series A, Mathematical and Physical Sciences* 230:463–501.

Pecina P. and Ceplecha Z. 1983. New aspects in single-body meteor physics. *Bulletin of the Astronomical Institutes of Czechoslovakia* 34:102–121.

ReVelle D. O. 1979. A quasi-simple ablation model for large meteorite entry: Theory versus observations. *Journal of Atmospheric and Terrestrial Physics* 41:453–473.

ReVelle D. O. 2001. Bolide dynamics and luminosity modeling comparisons between uniform bulk density and porous meteoroid models. Proceedings, Meteoroids 2001 Conference. ESA SP-495. Noordwijk: European Space Research and Technology Research Center. pp. 513–517.

ReVelle D. O. 2002. Fireball dynamics, energetics, ablation, luminosity, and fragmentation modeling. Proceedings, Asteroids, Comets, and Meteors 2002 Conference. ESA SP-500. Noordwijk: European Space Research and Technology Research Center. pp. 127–136.

ReVelle D. O. and Ceplecha Z. 2001. Bolide physical theory with application to PN and EN fireballs. Proceedings, Meteoroids 2001 Conference. ESA SP-495. Noordwijk: European Space Research and Technology Research Center. pp. 507–512.

Spurný P. 1994. Recent fireballs photographed in Central Europe. *Planetary and Space Science* 42:157–162.

Spurný P., Betlem H., Leven J. V., and Jeniskens P. 2000a. Atmospheric behavior and extreme beginning heights of the thirteen brightest photographic Leonid meteors from the ground-based expedition to China. *Meteoritics & Planetary Science* 35: 243–249.

Spurný P., Betlem H., Jobse K., Koten P., and Leven J. V. 2000b. New type of radiation of bright Leonid meteors above 130 km. *Meteoritics & Planetary Science* 35:1109–1115.